

Observations and Modelling of Tsunami Currents at the Port of Tauranga, New Zealand

Jose C. Borrero¹, Randall J. LeVeque², S. Dougal Greer¹, Sam O'Neill¹, and Brisa N. Davis²
¹eCoast Ltd., Raglan New Zealand; jose@ecoast.co.nz
²University of Washington, Seattle, WA, USA

Abstract

The March 11, 2011 Tohoku tsunami was recorded on five separate water level gauges and a current meter at the Port of Tauranga, New Zealand. As such it represents one of the most comprehensive instrumental data sets of a far-field tsunami affecting a major commercial port. In this paper we present a preliminary analysis of the measured current data, exploring the effect of tidal activity on the tsunami signal. We then model the tsunami in Tauranga using two numerical models; the MOST tsunami model using the ComMIT modelling framework, which relies in part on a database of pre-computed tsunami simulations, and the GeoClaw numerical model, using adaptive mesh refinement for the full simulation. Model results are compared in terms of their relative accuracy to the measured data as well other factors such as model run time, computational demand, model set up and ease of use. The results of this study will highlight the relative strengths between database driven and direct simulation approaches for the real time assessment of far field tsunamis in ports and harbours around the world.

Keywords: tsunami, numerical modelling, ports, currents, maritime hazards, long waves, MOST, GeoClaw

1. Introduction

The ability to measure, predict, and compute tsunami currents is of importance in risk assessment and hazard mitigation. Substantial damage can be done by high velocity flows, particularly in ports and harbours, even when the wave height is small and does not cause damaging inundation [5]. Until recently, few direct measurements of tsunami velocities existed to compare with model results. This paper presents a detailed comparison between measured and modelled water levels and current speeds for two tsunami propagation and inundation models - the MOST tsunami model using the ComMIT modelling framework, and the GeoClaw numerical model, using adaptive mesh refinement for the full simulation. Model results are compared in terms of their relative accuracy to the measured data as well other factors such as model run time, computational demand, model set up and ease of use.

2. The 2011 Japan Tsunami in New Zealand

The great Tohoku earthquake ($M_w = 8.9$) of March 11, 2011 (0546 UTC), occurred along the northern east coast of Honshu Island in Japan. The earthquake generated a devastating tsunami with the strongest effects observed in the near field close to the earthquake source and ultimately resulted in nearly 20,000 casualties and billions of dollars in damage [8]. In the far-field, the tsunami affected the entire Pacific Ocean with waves first arriving in New Zealand on the morning of 12 March [4].

The tsunami was recorded on 6 separate instruments located both inside and outside of Tauranga Harbour (Figure 1). These include two tide gauges (TAUT and Moturiki), three pressure

sensors (A Beacon, Tug Berth and Sulphur Point) maintained by the Port of Tauranga (POT) and an acoustic Doppler current meter at the entrance to the harbour that recorded current speeds.



Figure 1 Location map showing the entrance to Tauranga Harbour and the locations where tsunami data was recorded. Black box on inset map indicates extents of the 'A' level model grid. Port image extents correspond to those of the innermost 'C' level grids.

The filtered (tide signal removed) water level data (Figure 2) show that the maximum peak to trough

(P2T) tsunami height was in excess of 0.8 m on the Moturiki tide gauge. At A Beacon and locations inside the harbour, the tsunami heights were somewhat smaller.

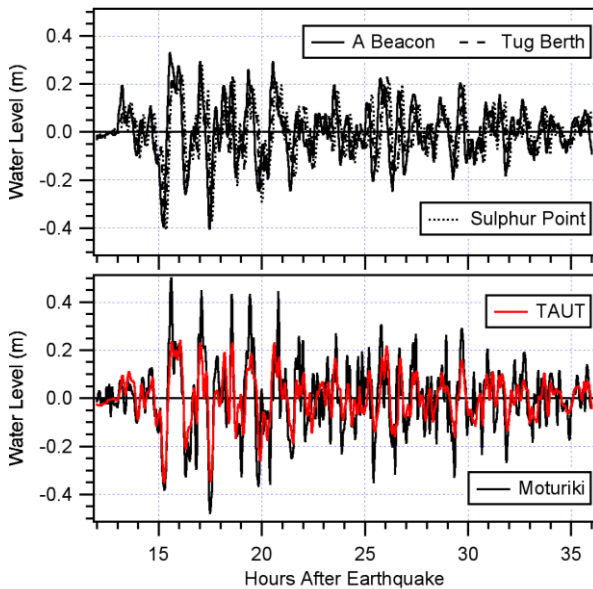


Figure 2 Measured water level data, filtered to remove the tide signal. (top) POT water level data, (bottom) TAUT and Moturiki tide gauges

2.1 Tsunami Currents

Maximum measured current speeds during the tsunami reached 2.5 m/s in the entrance to Tauranga Harbour (Figure 3). Removing the tidal component shows that the tsunami currents alone peak at approximately 1.0 m/s. Current speeds exceeded the 1.5 knot (0.77 m/s) threshold for the passage of large container ships through the entrance to Tauranga Harbour multiple times, however each of these occurred at times when the normal tidal currents would have also been in excess of that threshold. As a result, normal port operations were not disrupted and at no time did ships enter or exit the harbour during unsafe conditions.

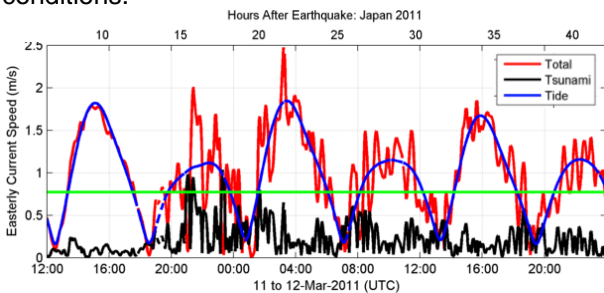


Figure 3 Measured currents during the 2011 Tohoku tsunami. Red: total measured current; blue: tidal currents and black: tsunami only, tidal component removed. Horizontal green line indicates 0.77 m/s (1.5 knots).

A scatter plot of the depth averaged U (east-west) and V (north-south) velocity data shows that the flood and ebb tidal flow directions at the deployment location are not aligned along the same axis. The flood currents flow towards the

south-east while the ebb currents flow towards the north-north-west.

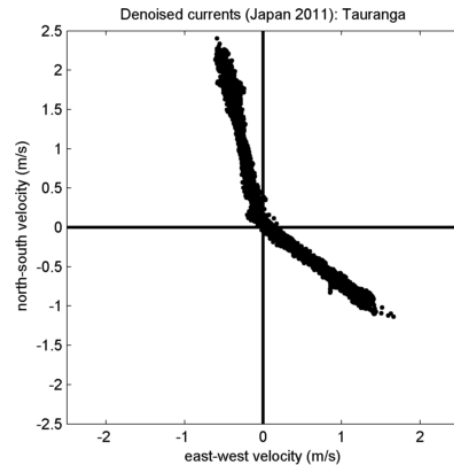


Figure 4 Scatter plot of depth averaged U (east-west) and V (north-south) velocity data. The lower limb is the flooding currents flowing towards the southeast while the ebb currents in the upper limb flow towards the north-northwest.

Plotting the U (east-west) and V (north-south) velocity components separately suggests that the current velocity components are subject to tidal modulation (Figure 5). It is clear looking at the east-west (U) component that during the ebb tide, when the tidal currents are principally aligned with the north – south axis and less along the east – west axis, tsunami generated currents are also reduced along the east-west axis, suggesting that the direction of the tsunami current is dependent on the direction of the tidal flow. This could be due to the bathymetric steering of the tidal wave causing the alignment of the shorter period tsunami wave.

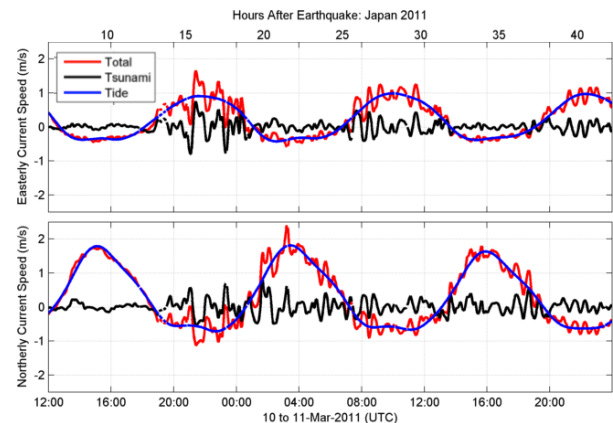


Figure 5 East-west (U, top) and north-south (V, bottom) velocity components.

3. Modelling

This study compares results from two numerical models. The first is the MOST (Method Of Splitting Tsunami) model [16] implemented through the Community Model Interface for Tsunamis (ComMIT) interface [17]. The backbone of the ComMIT system is a database of pre-computed deep water propagation results for tsunamis

generated by unit displacements on fault plane segments positioned along the world's subduction zones. Using linear superposition, the deep ocean tsunami propagation results from more complex faulting scenarios is created by scaling and/or combining the pre-computed propagation results from a number of unit sources. The resulting transoceanic tsunami propagation results are then used as boundary inputs for a series of nested near shore grids covering a region of interest.

The second model tested is the open source GeoClaw tsunami model [6]. This model has undergone extensive validation and verification [10, 3, 7, 11] using both synthetic test problems and real events for the comparison of water surface elevations and inundation. Most recently, GeoClaw was validated against tsunami currents measured in Hawai'i following the 2011 Tohoku tsunami [2].

The GeoClaw software implements high-resolution finite volume methods to solve the depth-averaged nonlinear shallow water equations. The finite volume methods implemented in GeoClaw are based on dividing the computational domain into rectangular grid cells and storing cell averages of mass and momentum in each grid cell. These are updated each time step by a high-resolution Godunov type method [9] that is based on solving Riemann problems at the interfaces between neighbouring grid cells and applying nonlinear limiters to avoid nonphysical oscillations. Block-structured adaptive mesh refinement (AMR) is used in GeoClaw to employ finer grid resolution in regions of particular interest.

4. Model Set-up

To facilitate a robust model comparison, wherever possible we attempted to use the same model bathymetry grids and initial condition. As noted above, for the MOST/ComMIT model, the trans-Pacific propagation results are computed on a 4-arcminute grid covering the entire Pacific Ocean and stored in an online database. Time series of water level and current speed are then extracted from this database, scaled appropriately and used as boundary conditions to drive the local simulation run over a 3-level nested grid covering the Bay of Plenty, Tauranga Harbour and the Port of Tauranga. Grids were constructed to provide adequate spatial coverage over the study site and fine enough spatial resolution to accurately resolve current speeds. Previous studies on modelled tsunami current speed using MOST suggest that 10 m grids are optimal for this purpose [1, 12]. For the purposes of sensitivity and performance testing, an additional fine resolution grid at 20 m spacing was also used over the Port area. The details of the computational grids are listed in Table 1.

For the GeoClaw modelling, a grid of 4' resolution derived from the ETOPO2 dataset was used for the transoceanic propagation. The same grid data used in the MOST/ComMIT model were implemented in to GeoClaw for the detailed simulations over Tauranga Harbour, although the finest computational mesh spacing used in this region was 1-arcsec (~30 m). Both models were run without the effect of tides and model output was compared to the de-tided tsunami data.

Table 1 Details of the modelling grids used in ComMIT. See Figure 1 for indication of spatial extents.

	dx,dy	nx, ny	max dt
A	~750 m	305x224	4.32 sec
B	~150 m	177x208	5.68 sec
C1	~10 m	600x901	0.52 sec
C2	~20 m	300x451	1.04 sec

4.1 Tsunami Source

Both the MOST and GeoClaw were initialised using the tsunami source model derived during the Tohoku event using measured tsunami data from DART tsunameters D21418 and D21419 (Figure 6). The source model is based on 100x50 km fault segments with different slip amounts applied to each segment. It is important to recognize that the use of real-time data from the DART tsunameters, enabled the development and distribution of this source model approximately 1.5 hours after the earthquake. Indeed this source was used to make timely threat assessments for communities on the US West Coast [18] and in New Zealand [4]. More details on the inversion process and tsunami source can be found in [15].

As with MOST, the GeoClaw simulations were initialised assuming an instantaneous deformation of the seafloor as predicted by elastic dislocation models [14] and using identical fault geometry and slip amounts as the MOST simulation. The computed sea floor deformation was then translated directly to the water surface as the model initial condition. Inspection of the computed deformation fields for each model show that they are nearly identical to one-another (Figure 7).

5. Model Results: MOST/ComMIT

The MOST simulation results (Figure 8) are consistent with measured data for positive amplitudes, however the model does not capture the large negative wave heights present in the data. This discrepancy is also evident when comparing modelled and measured current speeds. There are significant under-predictions, particularly when the tsunami wave heights are also under predicted. For portions of the time series where the modelled water levels match measured, currents speeds also match as evident from hour 16 to 20 in the time series. While the model does not match the measured data perfectly, it does provides a relatively good

representation of the observed tsunami arrival times, wave heights and wave periods.

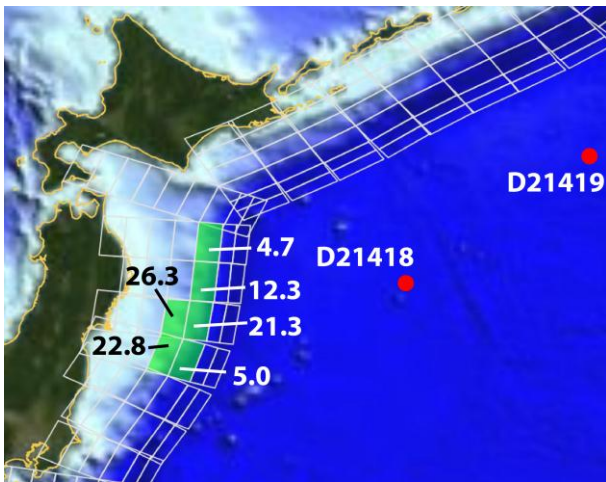


Figure 6 The tsunami source model used in this study. White rectangles are 100x50 km fault segments. Slip applied to each segment indicated in meters. Locations of DART tsunameters shown with red dots.

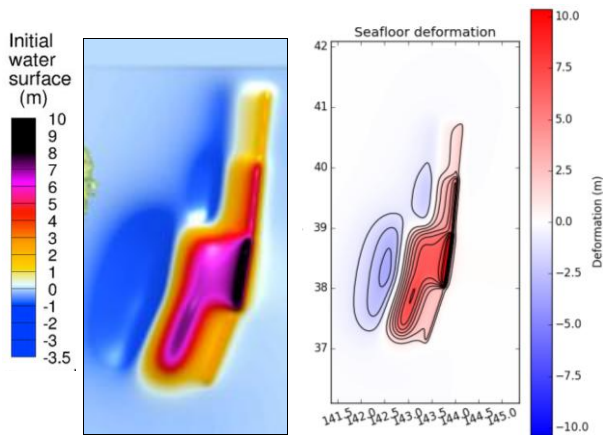


Figure 7 the MOST (left) and GeoClaw (right) initial water surface elevation/tsunami source model.

Comparison of the 10 m and 20 m grid results (Figure 8b) shows that the two sets are nearly identical with the exception of peaks where the models diverge. Though not presented here, water level predictions from the 20 m grid were also nearly identical to the 10 m grid model output. The similarity in the model results is encouraging particularly in light of differences in computational demand (discussed further below) between the 10 m and 20 m grid runs.

6. Model Results: GeoClaw

The simulation started on a coarse (4 deg.) grid covering the Pacific Ocean. The adaptive mesh refinement (AMR) is used to track the propagating waves on finer grids than other parts of the ocean. Higher levels of refinement are allowed or enforced around the region of interest (Tauranga Harbour in this case) only after the tsunami arrives.

A new adjoint-based AMR flagging procedure was used that facilitates choosing the refinement

regions in the Pacific to resolve only those parts of the wave that will arrive in Tauranga Harbour during the specified simulation. This capability is still under development and will appear in a future release of GeoClaw. A total of 6 levels of refinement were used, starting with 4-degree resolution on the coarsest level, with refinement ratios of 10, 6, 4, 10, 6 from one level to the next. Only 3 levels were allowed over most of the Pacific (to 4-arc minute resolution) and the remaining levels were used over increasingly focused regions around New Zealand. Level 6, with 1-arc second resolution, covered all of Tauranga Harbour.

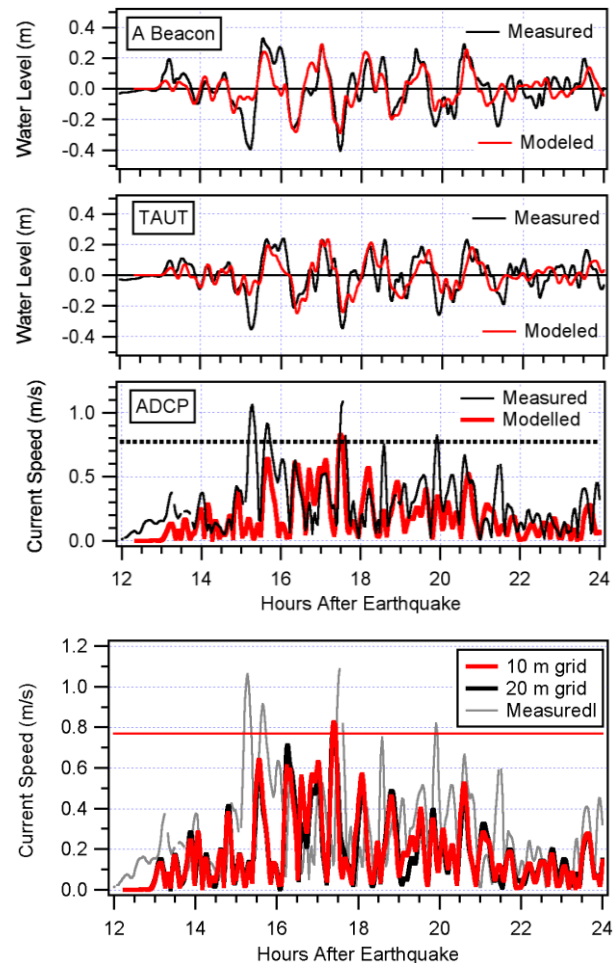


Figure 8 MOST/ComMIT model results. (A) Modelled vs. measured tsunami heights at A Beacon and TAUT and current speed at ADCP (B) Modelled current speeds for the 10 m and 20 m computational grids compared to measured data.

GeoClaw model results (Figure 9) were shifted 12 minutes later to better match the observed arrival time. Possible reasons for this offset are discussed in [2]. The results show reasonable agreement for the first few waves, but deteriorate after about 20 hours.

6.1 Computational Performance

The MOST/ComMIT simulation was run on a single processor of a 12-core desktop PC with a Windows 7 operating system. To run the model for

the first 12 hours of tsunami forcing in Tauranga Harbour required approximately 530 minutes of CPU time (8.8 hours). Reducing the inner grid resolution to 20 m however significantly reduced the model run time to 74 minutes (1.2 hours).

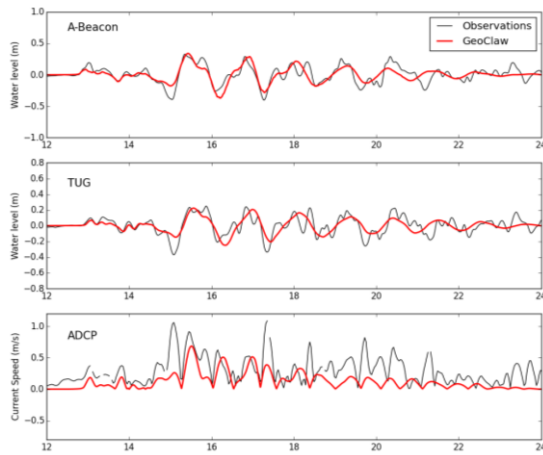


Figure 9. GeoClaw results. Modelled vs. measured tsunami heights at A Beacon and TUG and current speed at ADCP. Simulation results were shifted by 12 minutes.

Running the full GeoClaw simulation out to 30 hours post-earthquake required approximately 80 minutes on a quad-core laptop using the OpenMP option of GeoClaw. The fact that the tsunami was propagated from the source did not severely impact the performance due to the use of AMR. The first 12 hours of simulated time only required 3 minutes of computer time, and the bulk of the computational effort was consumed on the finer grids surrounding Tauranga Harbour, which were not introduced until 12.5 hours post-earthquake. To guide the refinement, the adjoint equation, linearized about the ocean at rest (essentially another shallow water equation), was first solved using GeoClaw on a single coarse grid and results stored and later used via interpolation. Solving this adjoint equation added 14 seconds to the total computing time.

7. Model to Measured Discrepancies

A major source of the discrepancy between the measured and modelled data likely results from the particular characterization of the tsunami source. Recall that the source model used here was optimized to match data recorded on two nearby tsunameters. As a result, the accuracy of the solution diminishes with azimuthal distance from the trench-perpendicular beam of maximum radiated tsunami energy. This is evident when comparing MOST model results to measured DART data at stations in the central and south Pacific (Figure 10) with the model consistently under predicting the magnitude of the leading wave trough. This feature is evident in both the MOST and GeoClaw results and undoubtedly contributed to the under-prediction of tsunami current speeds during the first (and largest) wave.

Additional discrepancies in the GeoClaw results may be due to lack of resolution within the harbour itself due to using ~30 m grids rather than 20 or 10 m as used in MOST.

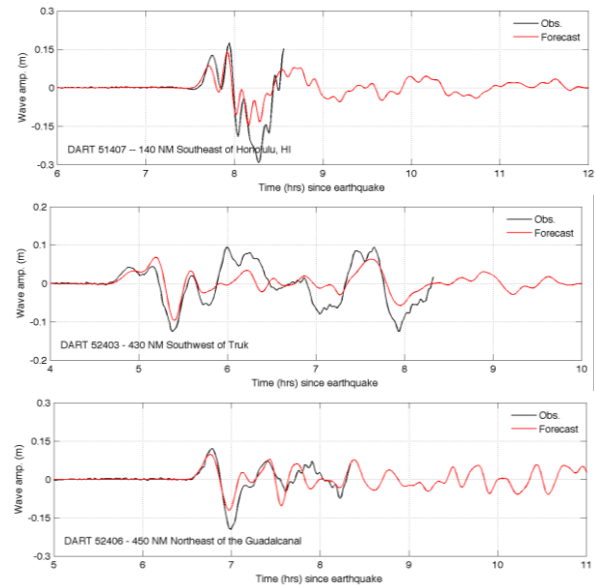


Figure 10 MOST model to measured DART data near Hawai'i (top) and in the southwest Pacific near Truk (mid) and Guadalcanal (bottom).

8. Summary and Conclusions

In a practical sense, the differences between measured and modelled for both simulations were relatively small. Indeed, the intent here was not to precisely model the effects of the Tohoku Tsunami, but rather to test the performance of two numerical models for the purposes of real time tsunami hazard assessments of tsunami hazards.

In this regard, both models performed well and accurately predicted – for the purposes of a real-time threat assessment – the arrival time and (other than the leading trough) the amplitudes and periods of tsunami waves for the first 12 hours of tsunami activity in Tauranga. In terms of current speeds, the models were less accurate, however, this is attributable primarily to the discrepancy in the height of the leading tsunami wave. Unpublished results show that when forced using the measured tsunami waveform recorded at A-Beacon, both models predict current speeds at the entrance to Tauranga Harbour with much greater accuracy [13].

In terms of model run time, the GeoClaw model required approximately 80 minutes. When added to the time needed to define the tsunami source, the GeoClaw assessment would have been ready less than 3 hours after the earthquake, leaving more than 9 hours to disseminate warning information and plan appropriate action. The ComMIT 10 m grid simulations took nearly 9 hours implying that hazard assessments would be ready only after 10.5 hours, leaving only 1.5 hour before

tsunami arrival. However, using a 20 m grid required only 74 minutes of computational effort with little appreciable change in model results.

Table 2 Model run times.

Model	Finest Grid Spacing (m)	Run Time (min)
GeoClaw	30 m	80
MOST	20 m	74
MOST	10 m	530

The ComMIT tool was specifically designed to integrate real time tsunami information and facilitate rapid accurate assessments of tsunami effects. As such it has the advantage of many years of intensive task-specific development that has resulted in a simple user interface and project work flow for setting up and running far field tsunami simulations. GeoClaw on the other hand is an open source model used for a wide range fluid dynamics applications. For inexperienced or first time users, compiling, setting up and running GeoClaw in a UNIX environment can be a daunting task. Once set up, the GeoClaw model offers nearly infinite flexibility and customisations, however this comes at the price of a relatively steep learning curve.

The results show that given a timely and accurate tsunami source, both models are able to provide robust estimated of tsunami wave heights for the purposes of a real-time threat assessment. The study also suggest the need to fine tune DART derived source mechanisms to improve the model results – particularly for tsunami currents – at far field locations situated off-axis from the main beam of tsunami energy. Continued refinements in the modelling methodologies and grid optimisation will allow for even more accurate tsunami hazard assessments.

9. Acknowledgements

The authors thank the Port of Tauranga, Dr. Willem deLange and Dr. Derek Goring for their cooperation and data sharing. Dr. Rob Bell provided the Moturiki tide gauge data. JCB and SDG were partially supported during this work by the Natural Hazards Research Platform of New Zealand's Ministry of Business Innovation and Employment (MBIE).

10. References

[1] Admire, A, Dengler, L, Crawford, G, Uslu, B, Borrero, J, Greer, S, Wilson, R (2014). Observed and Modeled Currents from the Tohoku-oki, Japan and other Recent Tsunamis in Northern California. *Pure Appl. Geophys.* doi:10.1007/s00024-014-0797-8

[2] Arcos, M, LeVeque, R (2015). Velocity Measurements Near Hawaii Compared to Model Simulations of the 11 March 2011 Tohoku Tsunami, *Pure Appl. Geophys.* 172, p. 849.

[3] Berger, M, George, D, LeVeque, R, Mandli, K. (2011). The GeoClaw software for depth-averaged flows with adaptive refinement. *Adv. Water Res.* doi:10.1016/j.advwatres.2011.02.016.

[4] Borrero, J., Bell, R, Csato, C, DeLange, W, Greer, D, Goring, D, Pickett, V, Power, W (2012). Observations, Effects and Real Time Assessment of the March 11, 2011 Tohoku-oki Tsunami in New Zealand, *Pure Appl. Geophys.* DOI 10.1007/s00024-012-0492-6

[5] Dengler, L, Uslu, B, Barberopoulou, A, Borrero, J, Synolakis, C. (2008). The Vulnerability of Crescent City, California, to Tsunamis Generated by Earthquakes in the Kuril Islands Region of the Northwestern Pacific. *Seismol. Res. Lett.* doi:10.1785/gssrl.79.5.608

[6] GeoClaw Development Team (2015). GeoClaw software, version 5.3.0. <http://www.geoclaw.org/>.

[7] González, F, LeVeque R., Varkovitsky, J., Chamberlain, P., Hirai, B., George, D. (2011). GeoClaw Results for the NTHMP Tsunami Benchmark Problems. <http://www.clawpack.org/links/nthmp-benchmarks/geoclaw-results>. GONZA

[8] IOC/UNESCO (2011). Japan Tsunami Bulletin No. 29, 30 September, 2011, 2 pp.

[9] LeVeque, R, (2002). Finite Volume Methods for Hyperbolic Problems. Cambridge University Press.

[10] LeVeque, R, George, D. (2007). High-resolution finite volume methods for the shallow water equations with bathymetry and dry states. In: Liu, P, Yeh, H, and Synolakis (eds.) *Advanced Numerical Models for Simulating Tsunami Waves and Runup*, 10(43–73), <http://www.amath.washington.edu/rjl/pubs/catalina04/>.

[11] LeVeque, R, George, D, Berger, M (2011). Tsunami modeling with adaptively refined finite volume methods. *Acta Numerica*, doi:10.1017/S0962492911000043.

[12] Lynett, P, Borrero, J, Son, S, Wilson, R, Miller, K (2014). Assessment of the tsunami-induced current hazard. *Geophys. Res. Lett.* doi:10.1002/2013GL058680

[13] Lynett, P. (2015) Personal Communication

[14] Okada, Y (1985). Surface deformation due to shear and tensile faults in a half-space, *Bull. Seismol. Soc. Am.*, 75, 1135–1154.

[15] Percival, D, Denbo, D, Eble, M, Gica, E, Mofjeld, H, Spillane, M, Tang, L, and Titov, V (2010). Extraction of tsunami source coefficients via inversion of DART buoy data, *Nat. Haz.* doi:10.1007/s11069-010-9688-1.

[16] Titov, V, and González, F (1997). Implementation and testing of the Method of Splitting Tsunami (MOST) model, NOAA Tech. Memo. ERL PMEL-112.

[17] Titov, V, Moore, C, Greenslade, D, Pattiaratchi, C, Badal, R, Synolakis, C and Kanoglu, U (2011). A new tool for inundation modelling: Community Modeling Interface for Tsunamis (ComMIT). *Pure Appl. Geophys.* 168, 2121–2131..

[18] Wei, Y, Newman, A, Hayes, G, Titov, V, Tang, L (2014). Tsunami Forecast by Joint Inversion of Real-Time Tsunami Waveforms and Seismic or GPS Data: Application to the Tohoku 2011 Tsunami. *Pure Appl. Geophys.* doi:10.1007/s00024-014-0777-z